Chinese Physics Letters **40**, 057102 (2023) **Express Letter**

Augmenting Density Matrix Renormalization Group with Disentanglers

Xiangjian Qian(钱湘坚) and Mingpu Qin(秦明普)*

Key Laboratory of Artificial Structures and Quantum Control (Ministry of Education), School of Physics and Astronomy, Shanghai Jiao Tong University, Shanghai 200240, China

(Received 2 February 2023; accepted manuscript online 6 April 2023)

Density matrix renormalization group (DMRG) and its extensions in the form of matrix product states are arguably the choice for the study of one-dimensional quantum systems in the last three decades. However, due to the limited entanglement encoded in the wave-function ansatz, to maintain the accuracy of DMRG with the increase of the system size in the study of two-dimensional systems, exponentially increased resources are required, which limits the applicability of DMRG to only narrow systems. We introduce a new ansatz in which DMRG is augmented with disentanglers to encode area-law-like entanglement entropy (entanglement entropy supported in the new ansatz scales as l for an $l \times l$ system). In the new method, the $O(D^3)$ low computational cost of DMRG is kept (with an overhead of $O(d^4)$ and d the dimension of the physical degrees of freedom). We perform benchmark calculations with this approach on the two-dimensional transverse Ising and Heisenberg models. This new ansatz extends the power of DMRG in the study of two-dimensional quantum systems.

DOI: 10.1088/0256-307X/40/5/057102

The study of exotic phases and the phase transitions between them in strongly correlated quantum many-body systems is one of the largest challenges in condensed matter physics.[1–3] The main difficulty stems from the exponential growth of the Hilbert space dimension with the system size, which means that brutal force approach can only handle very small systems. Analytic solution to quantum many-body systems is very rare.[4–8] Thus, most studies of these systems rely on different types of numerical methods nowadays.[9–17]

Density matrix renormalization group (DMRG)[12–15,18] is the most successful numerical method for the study of one-dimensional (1D) quantum many-body systems[19,20] in the past decades. However, it is known that the physics in two dimensions (2D) is richer.[21–30] The direct application of DMRG to 2D systems is not as successful as the study of 1D cases. It was found that the required resource needs to increase exponentially with the system size in 2D if we want to maintain the accuracy.[31]

It was realized later that the wave functions obtained by DMRG are actually matrix product states (MPSs),[32] and the success of DMRG lies in the fact that the entanglement encoded in the wave-function satisfies the entropic area law[33–36] of 1D quantum systems. Nevertheless, MPSs fail to capture the entropic area law for 2D systems which has to be remedied by exponentially large bond dimensions. To overcome this difficulty, MPSs were generalized to high dimensions in the perspective of tensor network states (TNSs).[37,38] There is also effort to modify the MPS ansatz for 2D systems.[39] In TNSs, the wave function of a quantum many-body system is represented as the contraction of connected tensors with polynomial parameters in contrast to the exponentially large Hilbert space. Different types of TNSs were proposed in the past, like projected entangled pair states (PEPSs),[17,40–44] tree tensor network (TTN),[45–48] multiscale entanglement renormalization ansatz (MERA),[49–52] and projected entangled simplex states (PESSs).[53] It can be easily proven that 2D PEPSs, MERA, and PESSs can capture the entropic area law for 2D quantum systems[36,53,54] which makes them better wave-function ansatz for 2D systems. Progress in the understanding of exotic states in 2D has been made with these TNS-related methods before,[40,55–59] but the high computational complexity hampers wide applications of them in research of 2D systems. The typical cost of PEPSs is $O(D^{10})$,[60] where D is the bond dimension (we note that many attempts have been made to low the computation cost of PEPSs[40,61–63]) and $O(D^{16})$[51] for MERA, which makes the calculation with large bond dimension infeasible and limit the power of these methods. For practical reason, because the parameters in DMRG and MPS-based approaches are easy to be optimized and the computational cost is low, they are still widely used in the study of 2D (ladder or cylindrical) systems[64–69] by pushing the bond dimension to very large numbers, even though they cannot capture the entropic area law for 2D systems intrinsically.

In this work, we introduce a new MPS or DMRG based ansatz dubbed as fully augmented matrix product state (FAMPS) by generalizing the idea from augmented TTN (aTTN)[45] and fully augmented TTN (FATTN)[46] to MPS. The entanglement entropy encoded in both TTN and MPS are bounded by $\log D$, but MPS has a lower cost than TTN. In the FAMPS, the MPS is augmented with disentanglers to increase the entanglement encoded in the wave function. In the simplest scheme, where disentanglers are placed directly in the physical layer and span only two sites, it can be proved that the entanglement entropy captured in FAMPS scales as $l \ln d^2$ with l the measure of the cut with which the system is divided into two parts and

*Corresponding author. Email: qinmingpu@sjtu.edu.cn
© 2023 Chinese Physical Society and IOP Publishing Ltd

d is the dimension of local Hilbert space. Most importantly, the low, i.e., $O(D^3)$ computational cost in DMRG is maintained in FAMPS.

Fully Augmented Matrix Product States. An MPS is defined as

$$|\text{MPS}\rangle = \sum_{\{\sigma_i\}} \text{Tr}[A^{\sigma_1} A^{\sigma_2} A^{\sigma_3} \cdots A^{\sigma_n}]|\sigma_1\sigma_2\sigma_3\cdots\sigma_n\rangle, \quad (1)$$

where A is a rank-3 tensor with one physical index σ_i (with dimension d) and two auxiliary indices (with dimension D). Disentanglers are unitary matrices which transform the physical degrees of freedom of two sites. They are common building blocks in TNSs which can reduce the local entanglement in the studied system.[50,70] Following the strategy in Refs. [45,46], we can place an additional disentangler layer on the physical layer of the MPS to increase the entanglement in the wave-function as

$$|\text{FAMPS}\rangle = D(u)|\text{MPS}\rangle, \quad (2)$$

where $D(u) = \prod_m u_m$ denotes the disentangler layer. Figure 1(c) shows the diagrammatic representation of the FAMPS, where we can find that the FAMPS is a more entangled wave function ansatz than the MPS.[71]

As discussed in Ref. [46], there are two criteria or constraints when placing disentanglers. The first one is that there should be no two disentanglers sharing the same physical site. The other is to place more disentanglers in places where the entanglement the ansatz wave-function can host is small. The first criterion ensures a comparable computational complexity with its predecessor (with a factor of d^4 at the worst case). The second criterion is to make the entanglement distribute as uniform as possible in the whole system. More specifically, we want to ensure the least entanglement in the wave function for all different cuts as large as possible.

The special structure of the FAMPS suggests that the optimization process of the FAMPS can be divided into two steps. First, the disentanglers can be optimized using the standard Evenbly–Vidal algorithm.[72] Second, the rest of the tensors can be directly optimized with the traditional MPS or DMRG optimization procedure by solving eigenvalue problems.[12] The optimization of disentanglers and MPS tensors are performed alternatively for many times until the energy is converged. The details can be found in the Supplementary Materials. As discussed in the Supplementary Materials, the $O(D^3)$ cost of DMRG is kept in the FAMPS with an additional factor of d^4.

The arrangement of a 2D lattice to a 1D one in DMRG was extensively studied in the past.[48,73] In the DMRG calculation, different arrangements have small effect on the accuracy as will be shown later. However, the way a 2D lattice is arranged in a 1D one is crucial when augmenting the MPS with disentanglers, which determines the amount of entanglement the wave function can encode. In Fig. 1, we show three different ways to arrange the 2D lattice in a 1D one. The scheme in Fig. 1(a) is the most commonly used one in the literature. In this scheme, the entanglement is large if we cut the system horizontally, while only one bond is crossed if the system is cut vertically. This means that an MPS in the scheme of Fig. 1(a) can only encode an entanglement entropy $S \leq \ln D$. To augment MPS with disentanglers based on the scheme in Fig. 1(a), we need to place all the disentanglers [the dashed rectangulars in Fig. 1(a)] horizontally according to the two criteria mentioned above. Because we can only place $L/2$ disentangles horizontally in each column and the entanglement entropy contributed by each disentangler is maximally $\ln d^2$, the maximum entanglement entropy the FAMPS in Fig. 1(a) can encode scales as $L \ln d$.

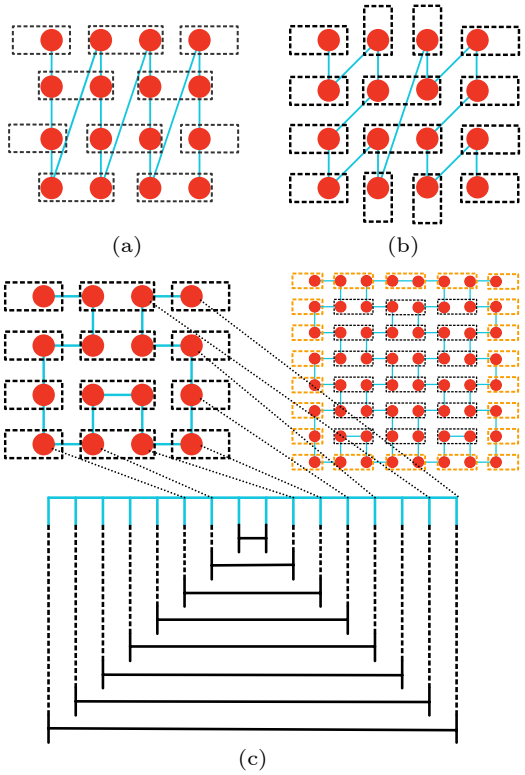

Fig. 1. Different schemes to arrange a 2D lattice into a 1D one in DMRG for periodic boundary conditions (PBCs). The disentanglers in the corresponding FAMPS are denoted as dashed rectangles. (a) The commonly adopted scheme for a 4×4 lattice. (b) A tree-type scheme for a 4×4 lattice (more details can be found in Ref. [46]). (c) A new scheme used in this work for 4×4 and 8×8 lattices and the corresponding one-dimensional representation of the 4×4 lattice where the dashed black lines indicate how disentanglers act on the MPS. The disentanglers at the edges denoted as dashed orange rectangles need to be rearranged for different boundary conditions. When augmented with disentanglers, the FAMPS encodes more entanglement in (b) and (c) than that in (a). See the main text for more discussion.

We have more efficient way to place the disentanglers. In Fig. 1(c), we introduce another scheme to arrange the 2D lattice in a 1D one. The entanglement in the MPS in Fig. 1(c) is more uniformly distributed than that in Fig. 1(a).[74] When augmented with disentanglers, the maximum entanglement entropy encoded in the FAMPS in Fig. 1(c) is $L \ln d^2$ which is twice the values in Fig. 1(a) and in the aTTN of Ref. [45]. Compared to Fig. 1(a), the number of crossed bonds with horizontal cut is reduced by a half, but even a small $D = d^4$ can support the $L \ln d^2$ entanglement entropy for these cuts. Actually Fig. 1(c) is not the only scheme to support the $L \ln d^2$ entanglement

entropy, another example is shown in Fig. 1(b), which is analyzed in Ref. [46] based on TTN. By placing the disentanglers appropriately, the arrangement following the Hilbert curve[48] can also support the $L \ln d^2$ entanglement entropy. In this work, we mainly focus on the scheme in Fig. 1(c).

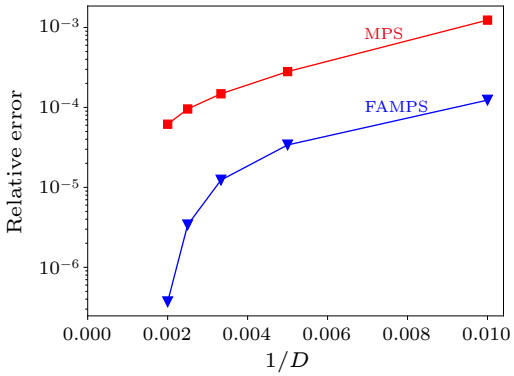

Fig. 2. Relative error of the ground state energy for FAMPS and MPS of the transverse Ising model near the critical point ($\lambda = 3.05$) for an 8×8 lattice with PBC. The scheme in Fig. 1(c) is used. The reference energy is the quantum Monte Carlo (QMC) result calculated by the stochastic series expansion (SSE) method with inverse temperature $\beta = 240$,[75,76] which is $-3.24163(1)$. Since our best energy of FAMPS, i.e., -3.2416288 (with $D = 500$), agrees with the reference energy within the error bar, the value of last point of FAMPS may be underestimated. We can find that the improvement of FAMPS over the MPS is about one order of magnitude.

Results on the Transverse Ising Model. We first test FAMPS in the two-dimensional transverse Ising model. The Hamiltonian of the transverse Ising model is

$$H_{\text{Ising}} = -\sum_{\langle i,j \rangle} \sigma_i^z \sigma_j^z - \lambda \sum_i \sigma_i^x, \tag{3}$$

where $\{\sigma_i^x, \sigma_i^z\}$ are Pauli matrices. In Fig. 2, we show the relative error of ground state energy from FAMPS and MPS simulations with $\lambda = 3.05$ (close to the critical point of the model). The scheme in Fig. 1(c) is used to map the 2D lattice into 1D. The system is with size 8×8 and with PBC. As shown in Fig. 2, we can find that the FAMPS is about one order of magnitude more accurate than the MPS, which is similar to the improvement of FATTN over TTN in Ref. [46].

Results on the Heisenberg Model. We also test the FAMPS on the 2D Heisenberg model whose ground state is more entangled than the transverse Ising model. The Hamiltonian of the Heisenberg model is

$$H_{\text{Heisenberg}} = \sum_{\langle i,j \rangle} S_i \cdot S_j, \tag{4}$$

where S_i denotes the spin of site i. We consider only nearest neighboring interactions. Here, we take advantage of the $U(1)$ symmetry[77] in our simulation. We take the numerically exact Quantum Monte Carlo results[10,40] as references. First, we calculate the ground state energy for 8×8 lattice with periodic boundary conditions to test the FAMPS with different schemes to arrange the 2D lattice in 1D. Figure 3(a) shows the relative error of the ground state energy as a function of bond dimension. We can find that the energies from the MPS without the disentangler layer have little differences for the three schemes in Fig. 1. This result agrees with the study in Refs. [48,73], which showed that different arrangements can lead to increased numerical precision but not significant for 2D systems. However, when augmented with disentanglers, the FAMPS results in Fig. 3(a) show that the differences in accuracy are significant for different arrangement schemes. As is expected, the FAMPS in Fig. 1(c) is more accurate than that in Fig. 1(a) because the entanglement encoded in the wave-function ansatz in Fig. 1(c) is larger. For the Heisenberg model, the improvement in accuracy is about half an order of magnitude.

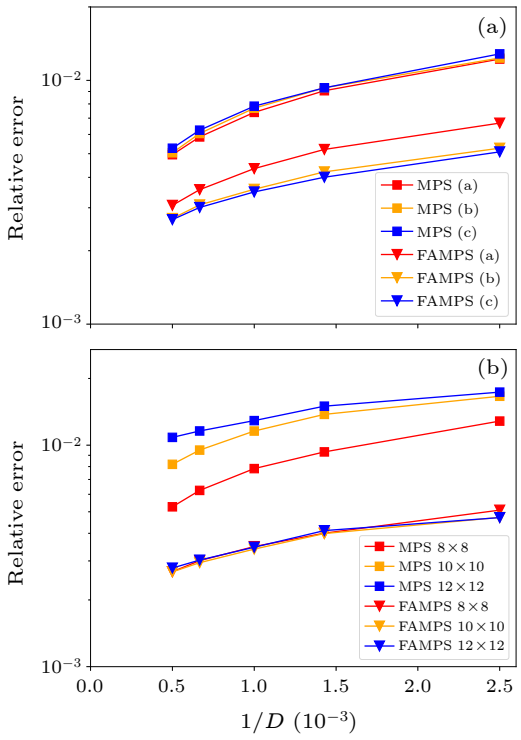

Fig. 3. Relative error of the ground state energy for FAMPS and MPS of the Heisenberg model with PBC. The reference energies are the numerically exact QMC results.[10] (a) We compare the results of different schemes in Fig. 1. Here (a), (b), and (c) in the legends denote the different schemes shown in Figs. 1(a), 1(b), and 1(c), respectively. We can see that the different schemes have little differences in DMRG energy. However, after augmented with disentanglers, the FAMPS in Fig. 1(c) gives lower energy than that in Fig. 1(a) as expected. (b) We compare the results of different lattice sizes using the scheme in Fig. 1(c). We can see that the FAMPS accuracy is maintained with the increase of lattice size while the MPS accuracy becomes worse as anticipated.

We then test FAMPS with larger sizes using the scheme in Fig. 1(c). In Fig. 3(b), we show the relative error of the ground state energy for lattice sizes 8×8, 10×10, and 12×12. The most important finding in these results is that the accuracy of FAMPS is maintained with the increase of lattice size, despite the accuracy of MPS decreases with the increase of lattice size as expected. This property

makes FAMPS a promising method in the study of two-dimensional systems in the future. We also test FAMPS for the Heisenberg model with open boundary conditions. We find that there exists a critical bond dimension after which the energies calculated by FAMPS and MPS are identical in the $U(1)$ symmetry imposed calculation (see the plot in the Supplementary Materials). This problem is caused by the absence of free parameters of disentanglers. The disentangler for spin 1/2 degree of freedom ($d = 2$) has one free parameter under $U(1)$ symmetry and no free parameter under $SU(2)$ symmetry. When the bond dimension exceeds the critical value, the state in $U(1)$ symmetry imposed MPS calculation nearly restores the $SU(2)$ symmetry. Thus, the extra disentangler layer has no effect, and FAMPS and MPS give the same results. The transverse Ising model has $Z(2)$ symmetry with two free parameters in the disentangler, which is the reason why there is no critical bond dimension in Fig. 2. The details of analyzing the number of free parameters in the disentanglers can be found in the Supplementary Materials.

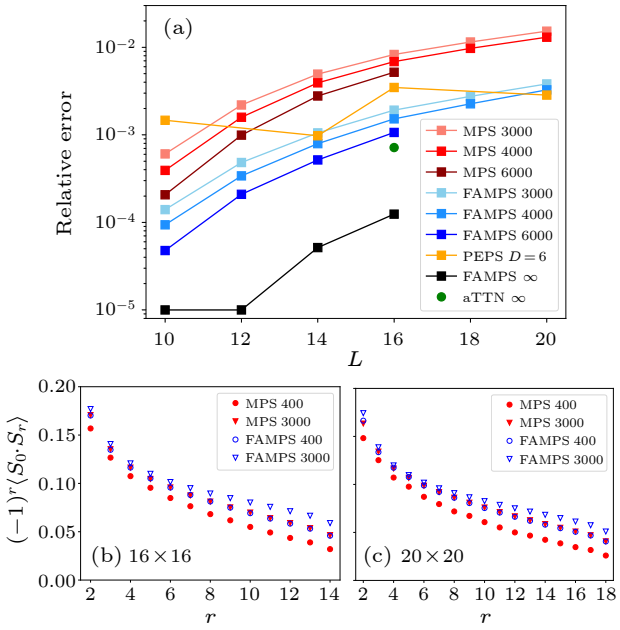

Fig. 4. (a) Relative error of the ground state energy for FAMPS, MPS, aTTN,[45] and PEPS[60] of the Heisenberg model on square lattice with sizes from 10×10 to 20×20 (squares and circles indicate open and periodic boundary conditions, respectively). The reference energy is the numerically exact results obtained by QMC in Refs. [10,40]. The black line is the extrapolated results for FAMPS at $D\to\infty$. For $L = 10$ and $L = 12$, because the extrapolated energies of FAMPS are exact within the error bar of QMC results, we set the relative errors of extrapolated FAMPS as 10^{-5}. From the plot, we can find that FAMPS is able to outperform PEPS for $L \le 20$. (b) and (c) The corresponding spin correlations along the horizontal direction for 16×16 and 20×20 systems. FAMPS is able to give the same accuracy with a nearly one tenth bond dimension ($D = 400$) compared with MPS ($D = 3000$).

To solve this problem, we block two sites into one to increase the number of free parameters of disentangler and impose $SU(2)$ symmetry in the calculation. Figure 4(a) shows the relative error of ground state energy calculated by MPS and FAMPS for different lattice sizes. We can find that the energies of FAMPS are lower than the PEPS results with bond-dimension $D = 6$ for $L \le 20$ in Fig. 4(a). When extrapolated to the infinite bond dimension limit for both FAMPS and aTTN, FAMPS is also more accurate than aTTN. Figures 4(b) and 4(c) show the corresponding spin correlations along the horizontal direction. FAMPS gives the same results as MPS with a nearly one tenth bond dimension for the correlation function.

Lastly, we show preliminary results of FAMPS on the more challenging J1–J2 Heisenberg model. We focus on the most difficult point with $J_2/J_1 = 0.5$. The comparison of ground state energy for an 8×8 system with PBC is listed in Table 1. We can find that the FAMPS energy with $D = 12000$ is more accurate than the previous DMRG energy with $D = 32000$, and FAMPS with $D = 24000$ gives the most accurate energy.

Table 1. The comparison of the ground state energy of the J1–J2 Heisenberg model ($J_2/J_1 = 0.5$) on an 8×8 square lattice with periodic boundary conditions.

Method	Energy per site
CNN	$-0.49639(2)$ [78]
RBM+PP	$-0.498460(6)$ [79]
DMRG $D = 24000$	-0.497961 [64]
DMRG $D = 32000$	-0.498175 [64]
VMC	$-0.49656(1)$ [80]
FAMPS $D = 12000$ (this work)	-0.498184
FAMPS $D = 24000$ (this work)	-0.498508

In summary, we have proposed a new ansatz, FAMPS, by augmenting an MPS with disentanglers. The FAMPS can encode area-law-like entanglement entropy for two-dimensional quantum systems and at the same time keeps the low $O(D^3)$ computational cost [with an overhead of $O(d^4)$]. We carry out benchmark calculations of the FAMPS on the 2D transverse Ising model near critical point and the 2D Heisenberg model. The FAMPS provides a useful approach to extend the power of DMRG for the study of difficult 2D problems.[64] The FAMPS can be generalized to encode more entanglement by placing multiple layers of disentangles to the MPS. The linearly scaled entanglement encoded in the FAMPS can also benefit many other MPS based approaches, e.g., the simulation of time evolution or the dynamic properties.[81–83] The FAMPS is also applicable to any other lattices by rearranging the studied system in a one-dimensional way.

Acknowledgments. The calculation in this work was carried out with Quimb[84] and TensorKit.[85] MQ acknowledges the support from the National Key Research and Development Program of China (Grant No. 2022YFA1405400), the National Natural Science Foundation of China (Grant No. 12274290), and the sponsorship from Yangyang Development Fund.

References

[1] Cabra D, Honecker A, and Pujol P 2012 *Modern Theories of Many-Particle Systems in Condensed Matter Physics.* Lecture Notes in Physics (Berlin: Springer) vol 843

[2] Wen X G 2007 *Quantum Field Theory of Many-Body Systems: From the Origin of Sound to an Origin of Light and Electrons* (Oxford: Oxford University Press)
[3] Marino E C 2017 *Quantum Field Theory Approach to Condensed Matter Physics* (Cambridge University Press, Cambridge)
[4] Berlinsky A J and Harris A B 2019 *The Ising Model: Exact Solutions* (Berlin: Springer International Publishing) p 441
[5] Dukelsky J, Pittel S, and Sierra G 2004 *Rev. Mod. Phys.* **76** 643
[6] Lieb E H and F Y W 1968 *Phys. Rev. Lett.* **20** 1445
[7] Qiao Y, Sun P, Xin Z, Cao J, and Yang W L 2020 *J. Phys. A* **53** 075205
[8] Zou H Y, Zhao E, Guan X W, and Liu W V 2019 *Phys. Rev. Lett.* **122** 180401
[9] Hirsch J E, Sugar R L, Scalapino D J, and Blankenbecler R 1982 *Phys. Rev. B* **26** 5033
[10] Sandvik A W 1997 *Phys. Rev. B* **56** 11678
[11] Huggins W J, O'Gorman B A, Rubin N C, Reichman D R, Babbush R, and Lee J 2022 *Nature* **603** 416
[12] White S R 1992 *Phys. Rev. Lett.* **69** 2863
[13] White S R 1993 *Phys. Rev. B* **48** 10345
[14] Schollwöck U 2005 *Rev. Mod. Phys.* **77** 259
[15] Schollwöck U 2011 *Ann. Phys.* **326** 96
[16] LeBlanc J P F, Antipov A E, Becca F *et al.* (Simons Collaboration) 2015 *Phys. Rev. X* **5** 041041
[17] Cirac J I, Pérez-García D, Schuch N, and Verstraete F 2021 *Rev. Mod. Phys.* **93** 045003
[18] Stoudenmire E and White S R 2012 *Annu. Rev. Condens. Matter Phys.* **3** 111
[19] Stoudenmire E M, Wagner L O, White S R, and Burke K 2012 *Phys. Rev. Lett.* **109** 056402
[20] Hida K 1999 *Phys. Rev. Lett.* **83** 3297
[21] Nakano H, Minami Y, and Sasa S I 2021 *Phys. Rev. Lett.* **126** 160604
[22] Verzhbitskiy I A, Voiry D, Chhowalla M, and Eda G 2020 *2D Mater.* **7** 035013
[23] Astrakharchik G E, Kurbakov I L, Sychev D V, Fedorov A K, and Lozovik Y E 2021 *Phys. Rev. B* **103** L140101
[24] Dalla Piazza B, Mourigal M, Christensen N B, Nilsen G J, Tregenna-Piggott P, Perring T G, Enderle M, McMorrow D F, Ivanov D A, and Rønnow H M 2015 *Nat. Phys.* **11** 62
[25] Ludwig A W W, Poilblanc D, Trebst S, and Troyer M 2011 *New J. Phys.* **13** 045014
[26] Brooks M, Lemeshko M, Lundholm D, and Yakaboylu E 2021 *Phys. Rev. Lett.* **126** 015301
[27] Han C, Iftikhar Z, Kleeorin Y, Anthore A, Pierre F, Meir Y, Mitchell A K, and Sela E 2022 *Phys. Rev. Lett.* **128** 146803
[28] Arovas D, Schrieffer J R, and Wilczek F 1984 *Phys. Rev. Lett.* **53** 722
[29] Halperin B I 1984 *Phys. Rev. Lett.* **52** 1583
[30] Wilczek F 1982 *Phys. Rev. Lett.* **49** 957
[31] Liang S D and Pang H B 1994 *Phys. Rev. B* **49** 9214
[32] Östlund S and Rommer S 1995 *Phys. Rev. Lett.* **75** 3537
[33] Plenio M B, Eisert J, Dreißig J, and Cramer M 2005 *Phys. Rev. Lett.* **94** 060503
[34] Vidal G, Latorre J I, Rico E, and Kitaev A 2003 *Phys. Rev. Lett.* **90** 227902
[35] Srednicki M 1993 *Phys. Rev. Lett.* **71** 666
[36] Eisert J, Cramer M, and Plenio M B 2010 *Rev. Mod. Phys.* **82** 277
[37] Orús R 2019 *Nat. Rev. Phys.* **1** 538
[38] Bridgeman J C and Chubb C T 2017 *J. Phys. A: Math. Theor.* **50** 223001
[39] Lami G, Carleo G, and Collura M 2022 *Phys. Rev. B* **106** L081111
[40] Liu W Y, Huang Y Z, Gong S S, and Z C G 2021 *Phys. Rev. B* **103** 235155
[41] Scarpa G, Molnár A, Y G, García-Ripoll J J, Schuch N, Pérez-García D, and Iblisdir S 2020 *Phys. Rev. Lett.* **125** 210504
[42] Liao H J, Liu J G, Wang L, and Xiang T 2019 *Phys. Rev. X* **9** 031041
[43] Hubig C 2018 *SciPost Phys.* **5** 47
[44] Vanderstraeten L, Burgelman L, Ponsioen B, Van Damme M, Vanhecke B, Corboz P, Haegeman J, and Verstraete F 2022 *Phys. Rev. B* **105** 195140
[45] Felser T, Notarnicola S, and Montangero S 2021 *Phys. Rev. Lett.* **126** 170603
[46] Qian X J and Qin M P 2022 *Phys. Rev. B* **105** 205102
[47] Silvi P, Tschirsich F, Gerster M, Jünemann J, Jaschke D, Rizzi M, and Montangero S 2019 *SciPost Physics Lecture Notes* 8
[48] Cataldi G, Abedi A, Magnifico G, Notarnicola S, Pozza N D, Giovannetti V, and Montangero S 2021 *Quantum* **5** 556
[49] Bridgeman J C, O'Brien A, Bartlett S D, and Doherty A C 2015 *Phys. Rev. B* **91** 165129
[50] Vidal G 2008 *Phys. Rev. Lett.* **101** 110501
[51] Evenbly G and Vidal G 2009 *Phys. Rev. Lett.* **102** 180406
[52] Vidal G 2007 *Phys. Rev. Lett.* **99** 220405
[53] Xie Z Y, Chen J, Yu J F, Kong X, Normand B, and Xiang T 2014 *Phys. Rev. X* **4** 011025
[54] Verstraete F, Wolf M M, Perez-Garcia D, and Cirac J I 2006 *Phys. Rev. Lett.* **96** 220601
[55] Evenbly G and Vidal G 2010 *Phys. Rev. Lett.* **104** 187203
[56] Corboz P and Mila F 2014 *Phys. Rev. Lett.* **112** 147203
[57] Liao H J, Xie Z Y, Chen J, Liu Z Y, Xie H D, Huang R Z, Normand B, and Xiang T 2017 *Phys. Rev. Lett.* **118** 137202
[58] Zheng B X, Chung C M, Corboz P, Ehlers G, Qin M P, Noack R M, Shi H, White S R, Zhang S, and Chan G K L 2017 *Science* **358** 1155
[59] Liu W Y, Gong S S, Y B L, Poilblanc D, Chen W Q, and Z C G 2022 *Sci. Bull.* **67** 1034
[60] Lubasch M, Cirac J I, and nuls M C B 2014 *Phys. Rev. B* **90** 064425
[61] Xie Z Y, Liao H J, Huang R Z, Xie H D, Chen J, Liu Z Y, and Xiang T 2017 *Phys. Rev. B* **96** 045128
[62] Fishman M T, Vanderstraeten L, Zauner-Stauber V, Haegeman J, and Verstraete F 2018 *Phys. Rev. B* **98** 235148
[63] Qin M P 2020 *Phys. Rev. B* **102** 125143
[64] Gong S S, Zhu W, Sheng D N, Motrunich O I, and Fisher M P A 2014 *Phys. Rev. Lett.* **113** 027201
[65] Yan S, Huse D A, and White S R 2011 *Science* **332** 1173
[66] Qin M, Chung C M, Shi H, Vitali E, Hubig C, Schollwöck U, White S R, and S. Zhang (Simons Collaboration on the Many-Electron Problem) 2020 *Phys. Rev. X* **10** 031016
[67] Jiang H C and Kivelson S A 2021 *Phys. Rev. Lett.* **127** 097002
[68] Gong S, Zhu W, and Sheng D N 2021 *Phys. Rev. Lett.* **127** 097003
[69] Jiang S, Scalapino D J, and White S R 2021 *Proc. Natl. Acad. Sci.* **118** e2109978118
[70] Ran S J 2020 *Phys. Rev. A* **101** 032310
[71] By contracting the additional disentangler layer in Fig. 1(c) into the original MPS wave-function, the effective bond dimension for the resulting MPS is much larger than the original MPS. Thus, the FAMPS is a more entangled wave-function than the MPS.
[72] Evenbly G and Vidal G 2009 *Phys. Rev. B* **79** 144108
[73] Xiang T, Lou J, and Z S 2001 *Phys. Rev. B* **64** 104414
[74] We can still easily find a vertical cut which crosses only one bond, but the number of these cuts is smaller
[75] Syljuåsen O F and Sandvik A W 2002 *Phys. Rev. E* **66** 046701
[76] The calculation of SSE QMC is performed with IsingMonteCarlo package at https://github.com/Renmusxd/IsingMonteCarlo
[77] Singh S, Pfeifer R N C, and Vidal G 2011 *Phys. Rev. B* **83** 115125
[78] Choo K, Neupert T, and Carleo G 2019 *Phys. Rev. B* **100** 125124
[79] Nomura Y and Imada M 2021 *Phys. Rev. X* **11** 031034
[80] Hu W J, Becca F, Parola A, and Sorella S 2013 *Phys. Rev. B* **88** 060402
[81] Paeckel S, Köhler T, Swoboda A, Manmana S R, Schollwöck U, and Hubig C 2019 *Ann. Phys.* **411** 167998
[82] Bañuls M C, Hastings M B, Verstraete F, and Cirac J I 2009 *Phys. Rev. Lett.* **102** 240603
[83] White S R and Feiguin A E 2004 *Phys. Rev. Lett.* **93** 076401
[84] Gray J 2018 *J. Open Source Software* **3** 819
[85] The $SU(2)$ symmetry code is developed with TensorKit package at https://github.com/Jutho/TensorKit.jl